CHAPTER 12

Solar-Climatic Cycles in the 4,190-Year Lake Saki Mud Layer Thickness Record

J. Xanthakis, I. Liritzis and C. Poulakos

Research Center for Astronomy and Applied Mathematics, Academy of Athens
14 Anagnostopoulou Street, Athens 106 73, Greece

ABSTRACT: Spectrum analysis methods (Fourier, Maximum Entropy, Power spectrum, successive approximations) have been applied to Lake Saki, Crimea, decadal mud layer thickness record since 2,300 years BC. The results obtained indicate several quasi-periodicities which superimpose upon each other, ranging between 25–1,000 years, which are attributed to solar-climatic cycles found in other proxy solar-climatic time-series.

INTRODUCTION

Lake Saki (Crimea) Data Record

A series of annual layers going back to 2300 BC in the mud deposits of a salty lake, Lake Saki, on the west coast of the Crimea (45°1′N, 33°5′E) has been measured (SCHOSTAKOWITSCH, 1934). These original data are reproduced in LAMB (1977), who has also converted them to rainfall scale suggested by BROOKS (1949), and thus produced rainfall variations in the Crimea since about 2300 BC (Figure 16.24 in LAMB, 1977, p. 408) (see Figure 7).

The layers are presumed mainly due to the run-off from the land caused by the heavier rainstorms; but most of the layers are only a few millimeters thick, and some may have been missed in the counting. This record suggests: (a) that cyclic variations occur, (b) that between AD 800 and 1250 represented a temporary return to moister conditions rather as they were in that area before 2000 BC, both being times of marked wetness setting in western and northern Europe.

In general, the implied wetness variations show some parallel with those which are thought to have occurred in central Asia and more often opposed to those over northern and central Europe.

A number of interesting and possibly important aspects appear in the variations of mud layer thickness. Some major sharp changes in the century-length regimes have occurred which may be a valuable signal of climatic change (even though such a change did not follow a periodic order or recurrence).

In the present work, spectrum analysis has been applied to this record. A detailed statistical analysis and use of various tests which examine stationarity has been made. The overall aim to model the Lake Saki mud layer thickness with regards to its ordered or random nature of variation suggests non-stationary periods of recurring fluctuations, that is, a sporadic, perhaps chaotic response of the mud layer thickness variation that has occurred throughout the past 4,200 years. The irregular behaviour amongst others is rather due to the hard to predict heavy rainstorms and the extreme persistent occurrences of blocking of the westerlies (large stationary anticyclones or cyclones) in the sea or of the northern hemisphere between 20° and 80° E.

The data records present the decade mean thickness (mm) of the yearly mud layers, 2300 BC–1890 AD comprising of $N = 420$ data points.

METHODS OF SPECTRAL ANALYSIS

Five different spectrum analysis methods were applied: (a) The Fourier periodogram (FFT); (b) the Maximum Entropy (MESA); (c) the Blackman-Tukey smoothed power spectrum method; (d) the power spectrum analysis attaching significance levels (MITCHEL, 1966); and (e) the "successive approximation" method, which locates the periods obtained by the four methods and defines their amplitudes. This also serves as a quantitative test of stationarity.

Fourier (FFT)

The raw data were detrended by subtraction of their mean. The residuals were analysed by FFT (Figure 1). The power spectrum density (PSD) gives many narrow sharp peaks two to six times above background. These peaks range between 20–250 years. The low frequency peak at 0.02 c/yr represents the half length of the record, an expected property of FFT analysis.

The quasi-periodic terms are: 21, 23, 25, 27, 30, 33, 38, 45, 62, 67, 91, 125, 250 (and 2,000) years. The nearly symmetric (tooth-saw) appearance of the peaks may imply presence of quasi-periodicities with variable length. This indication was further tested by smoothing the time-series with a 5-term moving average.

The FFT of the detrended record, after the subtraction of this smoothing, gave several common peaks with those of earlier analysis, but the much sharper peaks occasionally forming groups. (Figure 2). Thus, the 21-yr sharp peak sits on a multiline band between 20–22 yr. The 27 and 28 yr peaks overlay on a multiline band between 26–29 yr. Similarly, for the 44-yr (42–45); the 62, 65 and 72-yr (61–73) and the 125 and 154 yr (100–165). Thus, the variability in the obtained quasi-periodic peaks is also evidenced in the smoothed and detrended new time-series, which, moreover, groups the multiplets of Figure 2, providing as such a more representative variance spectrum for the variation of the original, raw, time series.

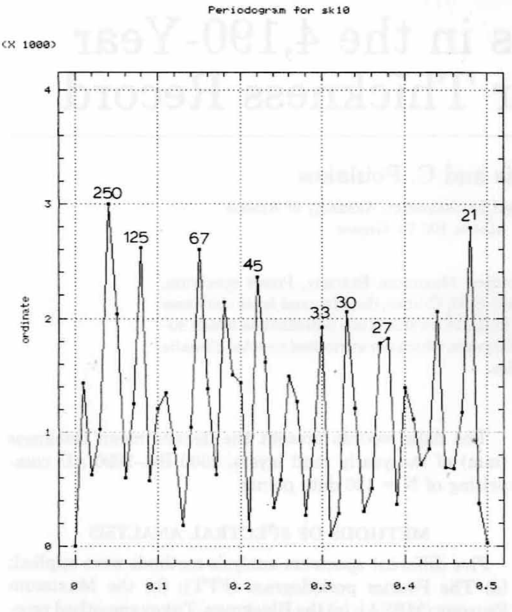

Figure 1. FFT periodogram analysis of Lake Saki 10-yr mud layers thickness record and main periods in years.

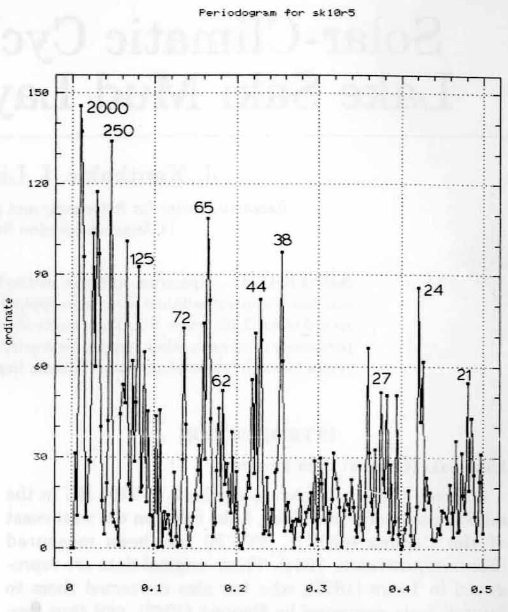

Figure 2. FFT periodogram analysis of Lake Saki 10-yr mud layers thickness detrended by a 5-terms moving average and main periods in years.

It seems that, so far, the mud layer thickness of Lake Saki displays variable quasi-periodicities, superimposed on each other, which form a kind of "network". Noteworthy is the estimated auto-correlation of the original record, detrended by subtraction of its mean value. Although the coefficients are quite small, they tend to wave in cycles of 60–70 yr, a quasi-period obtained also with the FFT.

An alternative smoothing of the raw data was also made for FFT. The mean value of each century was computed by "successively approximating" the century mean variations of the decadal values, with sinusoidals of defined position, length and amplitude (successive approximations method, see below). This computed century mean (C100 comp) was subtracted from each measured 10 yr mean thickness value (C10 meas). This C100, comp. has been estimated equal to

$$C_{100}^{\text{comp.}} = 13.8 + A \sin\frac{2\pi}{1{,}000}t + a \sin\frac{2\pi}{600}t + b \sin\frac{2\pi}{400}t + c \sin\frac{2\pi}{300}t \qquad (1)$$

where A, a, b and c are constant coefficients given in Table 4 and the 300, 400, 600, 1,000 years represent quasi-periodic terms.

The equation (1) represents the measured mud layer thickness data with an accuracy of 98%; it was formed by successive approximation of trigonometric functions by

Table 1. *MESA periodicities per different filter lengths F = 35–70 for the 1st half of the record (300 BC–1890 AD) and for the 2nd half of the record (2300 BC–210 BC). In parentheses are the low variance peaks.*

Filters	Periodicities in Years										
	1st half (300 BC–1890 AD)										
35	222		143		77	62, 5	45, 4	40		26	24	22
50	222	154		125	77	62, 5	45, 4	40		(26)	24	22
60	222	154		125	77	62, 5	45, 4	40	31	26	24	22
70	225			125		62, 5	45, 4	40			24	22
	2nd half (2300 BC–210 BC)										
25				125		62, 5	45, 4			27		21
50	250			125		62, 5	45, 4		(29)	(27)		(21)
70	250			125		62, 5	45, 4		29	27		21
88	250			125		62, 5	45, 4		29	27		21

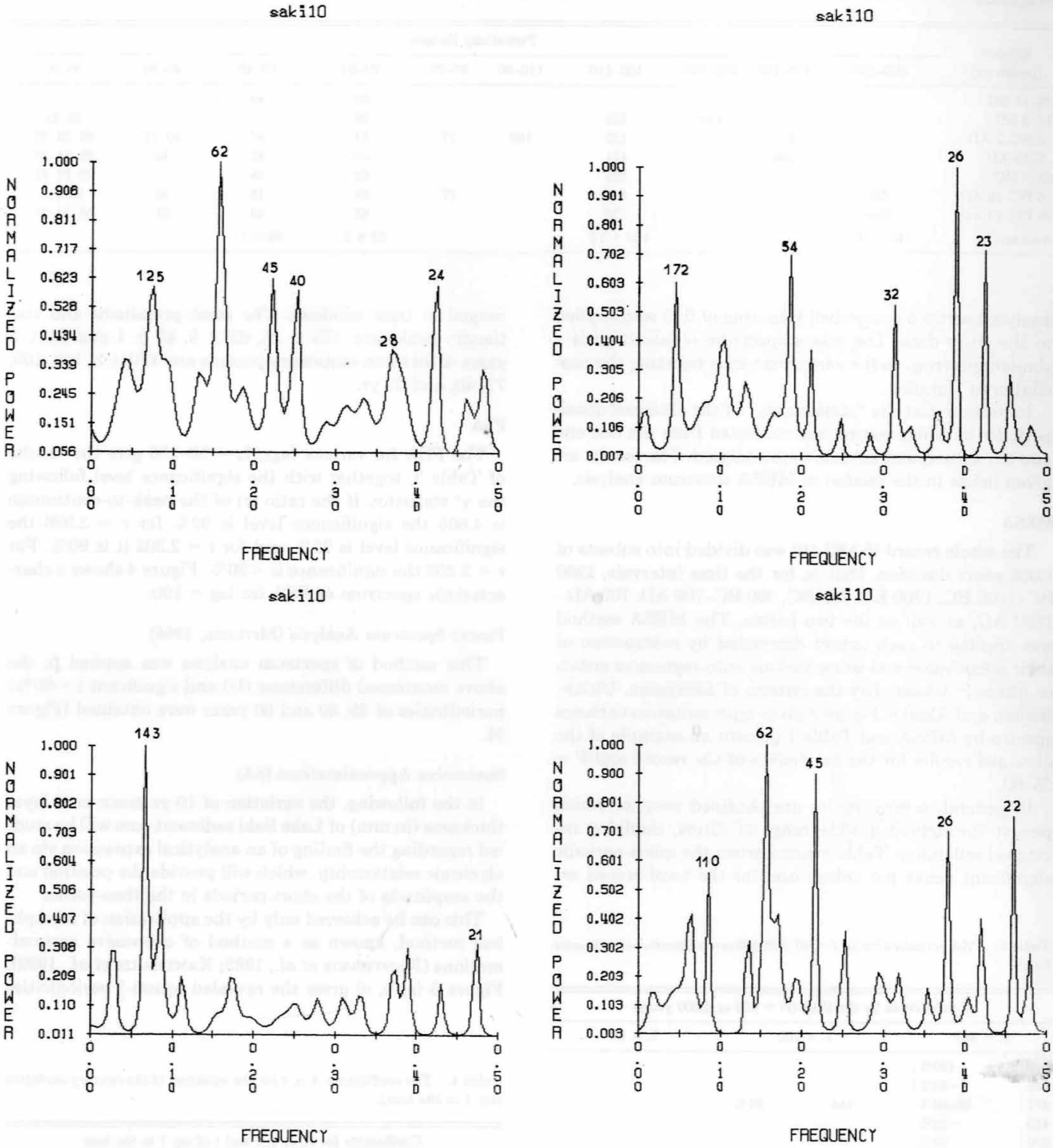

Figure 3. MESA spectra. (top left) all data, F = 40, (bottom left) data for 2300–1300 BC, F = 33, (top right) data for 1300 BC–300 BC, F = 38, and (bottom right) for 300 BC–1900 AD, F = 44.

gradual fitting of the time-series. The aim of this fitting was the analytical expression of the mean 100-yr data with the help of an analytical function. In this way the long term periodic terms of 300, 400, 600 and 1,000 years were subtracted.

The differences, D = C10, meas. − C100, comp., were tapered at both ends (10% of data or 0.1) and were analysed by FFT. The obtained periodic terms are similar in appearance with that smoothed with 5-term moving average and comprise of the following bands: 20–22, 24, 26–28, 38, 42–44, 57–60, 75, 100–145, 200–220 years. Furthermore, to test any effect of Hanning in both ends of the

Table 2. *MESA periodicities per subsets of around 1,000 years length as well as for all data and the two halves. The periodicities have been arranged in windows.*

Subsets (centuries)	Periodicity Ranges 200–250	170–150	150–130	130–110	110–90	90–70	70–50	50–40	40–30	30–20
23–13 BC							68	44		
13–3 BC			143	125			59			26 21
3 BC–7 AD		172		125	100	77	54	47	40 32	26 23 22
7–19 AD		166		111			63	45	40	26 24 22
23–3 BC				125			63	45		29 27 21
3 BC–19 AD	222			125		77	63	45	40	24 22
23 BC–19 AD	250			125			63	44	31	28 24 21
Average	240 ± 10			123 ± 10			62 ± 5	45 ± 1		

analysed series a cosine-bell (tapering of 0.1) was applied to the 10-yr data. The power spectrum obtained gives a similar spectrum to the earlier one thus rejecting the possibility of Hanning.

In order to test the "stationarity" of the obtained quasi-periods the whole record was truncated from the one end and the subsequent subsets were analysed. The results are given below in the section of MESA spectrum analysis.

MESA

The whole record (SAKI 10) was divided into subsets of 1,000 years duration, that is, for the time intervals, 2300 BC–1300 BC, 1300 BC–300 BC, 300 BC–700 AD, 700 AD–1890 AD, as well as the two halves. The MESA method was applied to each subset detrended by subtraction of their mean value and using various auto-regressive arders or filters F, which obey the criteria of Berryman, Ulrich-Bishop and Akaike. Figure 3 gives representative variance spectra by MESA and Table 1 present an example of the obtained results for the two halves of the record and F = 25–90.

In general, several cycles are obtained most of which persist throughout a wide range of filters, implying increased reliability. Table 2 summarises the quasi-periodic significant peaks per subset and for the total record arranged in time windows. The most prominent and stationary peaks are: 125 ± 25, 62 ± 5, 45 ± 1 and 24 ± 3 years. Other non-stationary periods are: 170 ± 3, 143, 100, 77, 40, and 32 yr.

Table 3. *PSA periodicities for L = 50, 100, 380 and respective significance levels.*

Periodicities by the PSA (N = 420 or 4,200 years) L = 380		L = 100		L = 50	
660	(90%)				
563	(~99%)				
447	95–99%	444	97%		
410	~99%				
330	99%				
250	90%	250 ± 25	90%	250	97%
230	99%				
214	99%				
185	(99%)	190	<90%		
146	99%	148	95%		
120–130	99%	125	99%	125	99%
79–80	97%	78–87	99%	83 ± 3	95%
64	99%				
58	99%				
52	90%	52 ± 1	99%	52	<90%
50–51	99%				
47	99%	47	>99%	47	~99%
41–42	95–99%	41–43	~95%	41	90%

PSA

The PSA for various lags, L = 50–380 give the results of Table 3, together with the significance level following the χ^2 statistics. If the ratio (r) of the peak-to-continuum is 4.605 the significance level is 99% for r = 2.996 the significance level is 95% and for r = 2.302 it is 90%. For r < 2.302 the significance is <90%. Figure 4 shows a characteristic spectrum of PSA for lag = 100.

Power Spectrum Analysis (Mitchel, 1966)

This method of spectrum analysis was applied to the above mentioned differences (D) and significant (> 95%) periodicities of 25, 40 and 60 years were obtained (Figure 5).

Successive Approximations (SA)

In the following, the variation of 10-yr mean mud layer thickness (in mm) of Lake Saki sediment core will be studied regarding the finding of an analytical expression via an algebraic relationship, which will provide the position and the amplitude of the short periods in the time-series.

This can be achieved only by the application of a graphical method, known as a method of successive approximations (Xanthakis *et al.*, 1985; Xanthakis *et al.*, 1992). Figure 6 (a, b, c) gives the revealed (quasi-) periodicities

Table 4. *The coefficients A, a, t for the equation of the century variation (eq. 1 in the text).*

Coefficients for A, a, b, c and t of eq. 1 in the text A	t	a	t
10	2500 BC–1500 BC	−3	700 BC–400 BC
8	2000 BC–1000 BC	3	900 AD–1200 AD
4	1500 BC–500 BC		1600 AD–1900 AD
3	1000 BC–0	4	1000 AD–1300 AD
−3	100 AD–600 AD		
2	1200 AD–1700 AD		
b	t	c	t
3	2400 BC–2000 BC	2	1200 BC–900 BC
	300 AD–900 AD		200 BC–100 AD
−3	1600 BC–1200 BC		

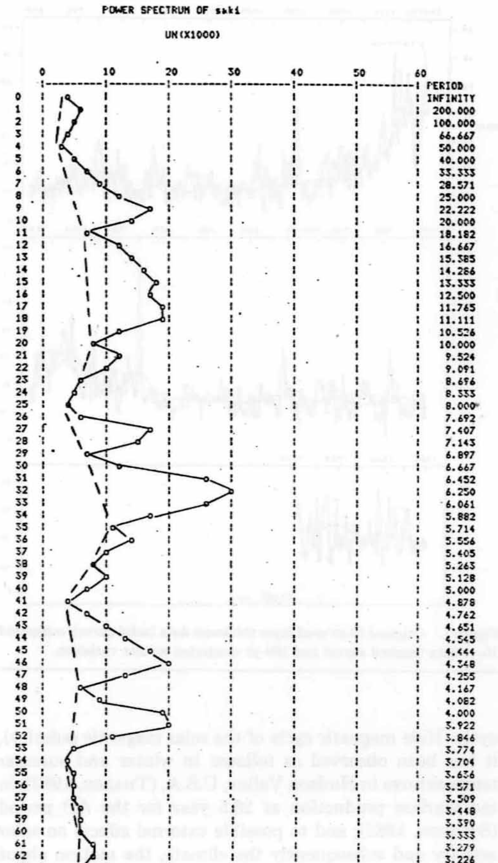

Figure 4. PSA spectrum for Lag = 100. The upper row indicates the periods in years $\times 10^{-1}$ the lower row is the lags and the dashed curve is the continuum (Background).

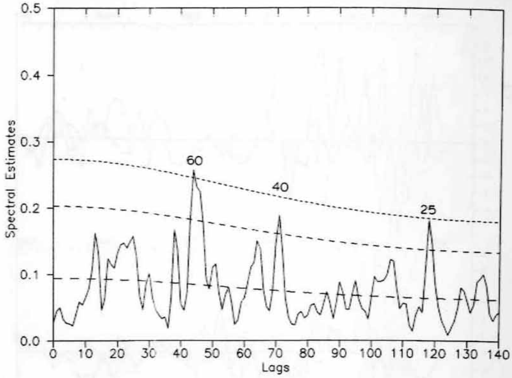

Figure 5. Power spectrum analysis (MITCHEL, 1966) where three significant periods appear at 25, 40 and 60 years with significance higher than 95%.

of 0–60 years, as well as, their positions for the time interval 2300 BC–1900 AD.

In several instances these periodic terms are superimposed upon each other or appear as quasi-periods, thus forming a network of periodicities. The later comply with the apparent chaotic behavior of the variation; being in fact a complex combination of several periodic terms (order emerging from non-linear or chaotic systems). Table 5 gives the amplitude and the position of the periodic terms revealed. Therefore, it is possible to express the mean 10-yr variation of mud layer thickness of Lake Saki by the following relationship.

$$C_{10}^{comp.} = C_{100}^{comp.} + a_1 \sin\frac{2\pi}{30}t + a_2 \sin\frac{2\pi}{40}t$$

$$+ a_3 \sin\frac{2\pi}{60}t + a_4 \sin\frac{2\pi}{80}t.$$

This equation fits the 10-yr original measured data with an accuracy of 95.8%. The standard deviation is equal to ± 0.58 mm and involves 29 degrees of freedom.

Figure 7 gives the representative variation of the mud layer thickness and includes the secular variation of C100, comp., the original 10-yr data (solid curve) and the computed 10-yr data (dashed curve) of C10, comp., for all the time interval.

DISCUSSION

All methods of spectrum analysis employed are complementary to each other and enhance the reliability of the detected periodic terms. These terms are present throughout the analysed time interval mainly as quasi-periods superimposed upon each other. Short-term 20–250 years and longer-term (> 500 year) periods have been obtained. The most significant (> 95%) and stationary periods are: 20–25, 45 ± 1, 62 ± 5, 120–130 and 200–250 years.

The PSA method instead of the 62 ± 5 yr gives a significant peak at around 80 years, some more above 250 years. The 20–25 year period resembles the double solar

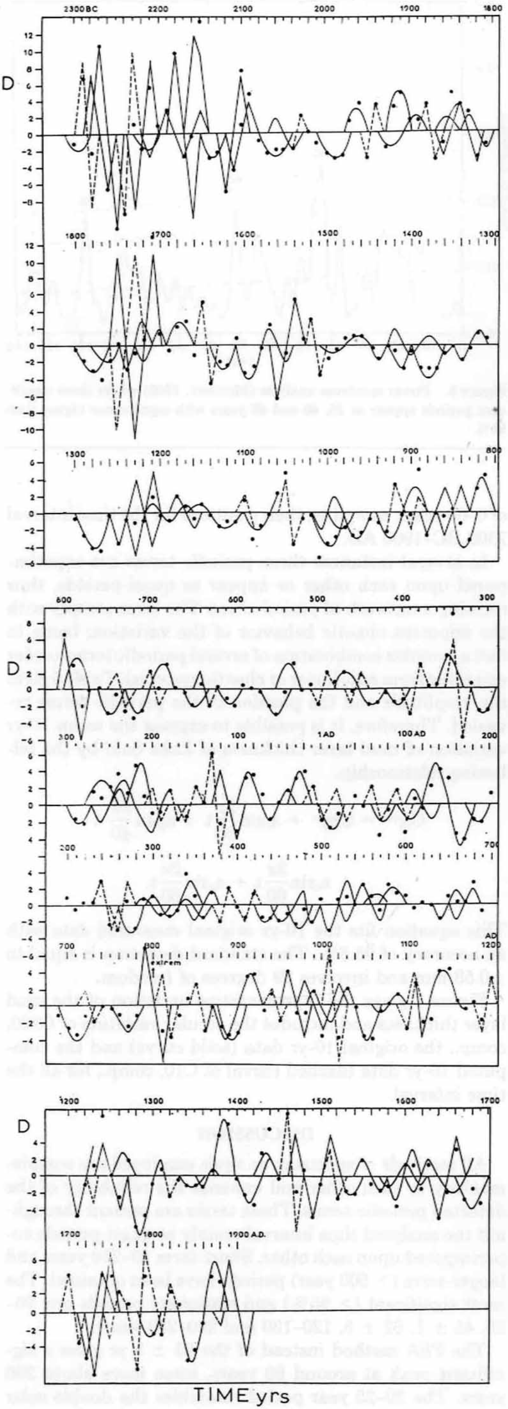

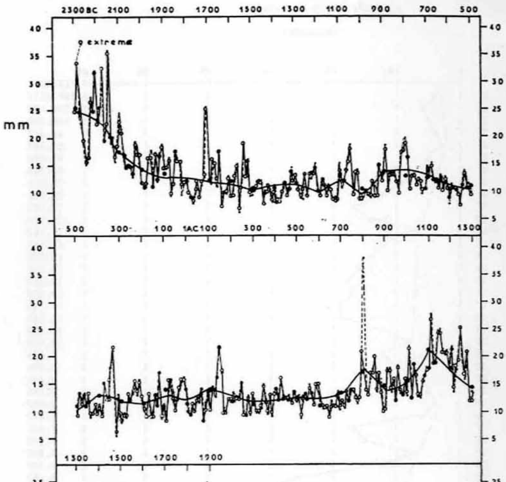

Figure 7. Original 10-yr mud layer thickness data (solid curve), computed 10-yr data (dashed curve) and 100-yr computed secular variation.

cycle (Hale magnetic cycle of the solar magnetic polarity), it has been observed as follows: in winter and summer temperatures in Hudson Valley, U.S.A. (THALER, 1987); in radiocarbon production as 26.5 year for the AD period (STUIVER, 1983); and to possible external effects on solar activity and subsequently the climate, the motion about the barycenter and the sun-centered Coriolis effects correlating with a 22-yr cycle.

The 45-yr cycle has been found in radiocarbon production, in ^{18}O and deuterium analyses of ice-cores glaciers on Greenland and Baffin island (JOHNSEN *et al.*, 1970) as follows: in summer storminess recorded by beach ridges back to more than 8,000 yr; also it appears as a frequency beat of Uranus/Saturn lap period of 45.387 yr, bringing to our attention the celestial mechanics aspects on the earth's climate and solar-terrestrial relationships.

Further, the 55–65-yr cycle has been reported for sunspots (SCHOVE, 1983) while it is also the apsides-perihelion cycle of 62.013 yr when the earth and sun respond to the variable force introduced by the moon's orbital fluctuation. Moreover, it has been yielded from several sets of D/H and

←

Figure 6. Successive approximations of $D = C_{10}^{meas} - C_{100}^{comp}$ for the time interval 2300 BC–1900 AD, where the short periodic terms between 20–60 years are located and their amplitudes estimated, (a) 2300 BC–800 BC, (b) 800 BC–1200 AD, (c) 1200 AD–1900 AD.

Table 5. *The coefficients of a_{1-4}* and t for the equation of computed 10-yr time-series (eq. 2 in the text).

Values of the parameters a_1–a_4 and t of eq. 2 in the text	
a_1	t, BC Period
9	2300–2330
−10	2250–2220
−2	2150–2180, 2060–2030, 910–880, 510–480, 470–440, 170–140
3	1890–1850, 1530–1500
5	1860–1630
2	1110–1080, 750–720, 710–630, 660–630, 210–180, 190–160
4	1060–1030
−3	940–910, 400–370, 1960–1930
6	350–320, 140–110
a_1	t, AD Period
2	20–40 BC, 930–960, 1110–1140, 1300–1330, 710–750
−2	150–90, 370–430, 470–500, 1870–1900
3	230–260, 840–870, 1500–1530
−3	250–280, 1090–1120, 1180–1210, 1220–1250, 1740–1770, 1800–1830
4	800–830, 1100–1130, 1690–1720
7	1000–1030, 1650–1680
−1	1350–1380
6	1450–1480
−7	1770–1800
a_2	t, BC Period
7	2290–2250, 810–770
11	2280–2240, 1760–1690, 1750–1720
9	2240–2200
10	2190–2150
−2	2220–2140, 2070–2030, 1730–1690, 1450–1410, 1350–1310, 1020–980, 70–30
−7	2130–2090
−4	2120–2080, 1260–1220
−3	1870–1800, 1260–1200, 890–850, 870–830, 2220–2140, 1750–1710
2	1580–1540, 1350–1310, 1190–1150, 2070–2030
−1	1410–1350
1	1220–1180
−5	1240–1200
4	130–90
−6	1570–1530
a_2	t, AD Period
−3	500–540, 1570–1610
−2	520–580, 630–670, 650–690, 1600–1640
7	780–820
4	950–990, 1240–1270, 1460–1520
3	970–1010, 500–540
2	980–1040, 1540–1580, 340–380
−4	1200–1240, 1710–1750
−5	1630–1670
1	280–320, 290–370, 1060–1100
−7	1720–1760
6	1880–1920
a_3	t, BC Period
−2	2230–2200, 1940–1820, 1780–1750, 1100–1070, 660–630, 620–590, 420–390, 300–270
−3	2150–2120, 1640–1610, 1430–1400, 980–950, 760–730, 730–670, 320–290
2	1870–1840, 480–420
−4	1610–1580, 850–820
−1	1510–1440
1	1170–1140
3	910–880, 550–520, 250–190, 1980–1950, 1690–1660
4	810–780, 100–70, 40–10, 800–770
5	230–200

Table 5. *Continued.*

a_3	t, AD Period
−3	1–30, 260–290, 460–490, 1400–1440, 1780–1810
−2	60–90, 90–120, 170–200, 420–450, 440–470, 1520–1550, 1640–1680
3	330–360, 1420–1450, 1250–1280
4	130–160, 1130–1160
1	550–580
2	570–600
−4	870–930, 880–910, 1030–1060, 1660–1700
7	1370–1400
−1	1570–1630, 1330–1360
−6	1830–1890
5	120–180
a_4	t, BC Period
−3	2080–2040, 2010–1930, 1800–1760, 570–530
−4	1400–1360, 1300–1260, 1020–980
a_4	t, AD Period
−3	690–770
−2	750–790

$^{18}O/^{16}O$ from *Cryptomeria Japonica* and Greenland ice core.

The ~80 yr cycle is the so-called Gleissberg solar cycle, which it does not persist throughout all the record but from MESA (Table 2) seems to exist in 300 BC–700 AD and in the second half (300 AD–1900 AD). The PSA gives the peak in the three lags (95–99%).

The ~125-yr cycle has been found also, in radiocarbon mainly during the second millenium AD and even in the whole period to some extent. The ~250-yr cycle is not so significant, but the ~200-yr cycle is strong in FFT and appears as 185 or 124 (99%) in PSA. This may be the auroral and sunspot cycle of 200 yr (Liritzis 1990; Xanthakis *et al.*, 1985) as well as, that found in radiocarbon (Neftel *et al.*, 1981; Schove, 1983) and tree-rings (Schove, 1983; Sonett and Suess, 1984), and in archaeomagnetic intensity (Liritzis, 1985).

Longer cycles exist but a longer period will need to be analysed before their significance can be assessed. For example, the PSA has revealed 330 yr (99%), 410 yr (99%) 447 yr (95–99%) and 563 yr (99%). It is worth noticing that the short periods have been found also in tree-ring width variation from a Cypress-tree in Parthenon, Athens (Liritzis and Kosmatos, 1994, in this volume).

In general, we have obtained cycles of solar-climatic and solar-planetary dynamics origin. It seems that various climate proxy time-series are characterized by significant oscillations which appear with variable length, amplitude and phase depending upon the geographical position. It is not necessary to find all these cycles in every geophysical/geological/physical time-series parameters analysed. In addition to their geographical position the terrestrial response to the several agents must be accounted for, which again has latitudinal and longitudinal effects.

CONCLUSION

We have applied several methods of spectrum analysis to the variation of the mean 10-yr mud layers thickness from Saki lake sediments core and several significant quasi-periodicities have been obtained ranging between 25–250 yr and long ones of 300, 400, 600 and 1,000 yrs. These cycles were located in the time-series and their amplitudes assessed. These are all either of solar, climatic or solar-planetary origin, all of which "beat" these pulses via the atmosphere (climate) and are recorded in the annual sedimentation rate of Lake Saki in Crimea.

LITERATURE CITED

BROOKS, C.E.P., 1949. *Climate Through the Ages.* London: Benn, 2nd edition, 395p.

FAIRBRIDGE, R.W. and SANDERS, J.E. 1987. The Sun's orbit AD 750–2050: Basis for new perspective on planetary dynamics and Earth-Moon linkage. *In:* RAMPINO *et al.* (eds.), *Climate, History, Periodicity and Predictability.* New York: Van Nostrand Reinhold Co., pp. 446–471.

JOHNSEN, S.J.; DANSGAARD, W., and CLAUSEN, H.B., 1970. Climatic oscillations 1200–2000 AD. *Nature,* 277, 482–483.

LAMB, H.H., 1977. *Climate: Present, Past and Future,* Vols. 1 & 2. London: Mathuen.

LIRITZIS, I. 1985. Maximum entropy and power spectrum analysis of geomagnetic intensity variations from archaeomagnetic data: Emphasis on the 200-yr period. *Earth, Moon, Planets,* 34, 235–249.

LIRITZIS, I. 1990. Evidence for periodicities in the auroral occurrence frequency since 300 AD and their implications. *PAGEOPH,* 133(2), 201–211.

LIRITZIS, I. and KOSMATOS, D., 1994. Solar-climatic cycles in a tree-ring sequence from Parthenon, Journal of Coastal Research. Special Issue No. 17.

MITCHEL, J. M., JR., 1966. The power spectrum and general principles of its application to the evaluation of non randomness in climatological series. Climate change, *WMO No. 195,* TP 1000, 33–47.

NEFTEL, A.; OESCHGER, H., and SUESS, H.E., 1981. Secular non-random variations of cosmogenic carbon-14 in the terrestrial atmosphere. *Earth and Planetary Science Letters,* 56, 127–147.

SCHOSTAKOWITSCH, W.B., 1934. *Bodenablagerungen der Seen und periodische Schwankungen der Naturerscheinungen.* (reprinted in English by C.E.P Brooks in Met. Magazine, 70, 134–138 (1935) from Memoirs of the Leningrad Hydrographic Institute.

SCHOVE, D.J. 1983. Sunspot Cycles. *Benchmark Papers in Geology* Series, vol. 68. New York: Van Nostrand Reinhold, 393p.

SONETT, C.P. and SUESS, H.R., 1984. Correlation of Bristlecone pine ring widths with atmospheric carbon-14 variations. A climate-sun relation. *Nature,* 308, 141.

STUIVER, M., 1983. The AD record of climatic and carbon isotope change. *Radiocarbon,* 25, 221.

THALER, J.S., 1987. Hudson valley reconstructed temperature data sets: History and spectral analysis. *In:* RAMPINO *et al.,* (eds.), *Climate: History, Periodicity and Predictability.* New York: Van Nostrand Reinhold, pp. 70–77.

XANTHAKIS, J.; LIRITZIS, I., and GALLOWAY, R.B., 1992. Periodic variation in natural radioactivity of lake Bouchet sediments. *Earth, Moon, Planets,* 59, 191–200.

XANTHAKIS, I.; LIRITZIS, I., and PETROPOULOS, B., 1985. Evidence for periodicities in the frequency occurrence of the Aurora Borealis since 300 AD. *Journal of Interdisciplinary Cycle Research,* 1, 2, 85–91.